Uncertainty Quantification of Inducer Eigenvalues using Conditional Assessment of Models and Modal Test of Simpler Systems

Andrew M. Brown, Ph.D.[a], Jennifer L. DeLessio[b], Timothy J. Wray, Ph.D.[c]

[a] Aerospace Engineer, NASA/Marshall Space Flight Center,
ER41/Propulsion Structural & Dynamic Analysis, Huntsville, AL 35812
[b] Propulsion Systems Analyst, JSEG/ESSCA – NASA/Marshall Space Flight Center,
ER41/Propulsion Structural & Dynamic Analysis, Huntsville, AL 35812
[c] Aerospace Engineer, NASA/Marshall Space Flight Center,
ER41/Propulsion Structural & Dynamic Analysis, Huntsville, AL 35812

ABSTRACT

The low pressure fuel pump inducer of the new Space Launch System RS25 core stage engine operates in a highly complex environment that substantially affects its modal characteristics. Some of the more important effects are fluid-added mass resulting from operation within a light liquid (Hydrogen), and the magnification of this effect due to tight tip clearance. Since higher order cavitation has been identified as a significant harmonic driver, knowledge of the natural frequency of potentially excitable modes is critical for safe operation, but this frequency cannot be measured during the severe operational environment. A comprehensive testing and analysis program has therefore been performed over the last four years to identify the nominal value and uncertainty of the frequency by modeling and testing two simpler structures in several configurations which share some of the characteristics of the operational inducer. This testing was used to assess and adjust modeling techniques and excellent correlation was achieved. Identification of the uncertainty in the inducer frequency itself was still problematic, however. This difficulty led to an investigation of Bayesian uncertainty quantification techniques, and to the application of the relatively simple technique of Multi-Variate Normal conditional distributions to calculate the inducer natural frequency uncertainty. Assumptions on prior distributions of uncertainty of the fluid-added mass and tip clearance effect are initially applied to models of each of the simple structures and the inducer itself, and these uncertainties are propagated to generate natural frequencies using design of experiments. Simple response surfaces are then created from this data in order to calculate a Covariance Matrix relating all of these natural frequencies. Finally, the results from modal test of the simple structures are considered to be observations and used to calculate the conditional variance of the desired inducer frequencies. As this method is less rigorous than more complicated Bayesian methods reported in the literature, a conservative factor is applied to the result, but the resulting uncertainty is still significantly less than originally estimated and will greatly assist certification of the inducer for use in the engine.

Keywords: Uncertainty Quantification, Structural Dynamics, Modal Test, Liquid Hydrogen, Bayesian Techniques, Model Updating

NOMENCLATURE

CB	Cantilever Beam
DOF	Degrees of Freedom
DOE	Design of Experiments
E	Young's Modulus
FS	Full-Scale
HOC	Higher Order Cavitation
HOSC	Higher Order Surge Cavitation

LH2	Liquid Hydrogen
LPFP	Low Pressure Fuel Pump
MAC	Modal Assurance Criterion
ND	Nodal Diameter
PDF	Probability Density Function
RT	Room Temperature
ρ_f	Fluid mass density
rv	Primitive Random Variable
SLS	Space Launch System
SSME	Space Shuttle Main Engine
SS	Sub-Scale
SSP	Simply Supported Plate
Ti	Titanium

INTRODUCTION

Liquid rocket engines are powered by the combustion of two propellants at very high pressure, a fuel and an oxidizer. Frequently, the fuel is liquid hydrogen (LH2). While the pressure can be provided by a very high-strength storage tank, usually this would be weight-prohibitive, so a turbopump or series of turbopumps are required to provide these extremely high pressures. The staged-combustion cycle of the RS-25 engine powering the core stage of NASA's Space Launch System, which is an adaption of the Space Shuttle Main Engines which operated successfully for 30 years, has low and high pressure fuel and oxidizer turbopumps. The low pressure fuel pump, which is fed directly by the fuel tank via ducting, uses an inducer to pressurize the liquid hydrogen fuel several hundred psi (Fig. 1).

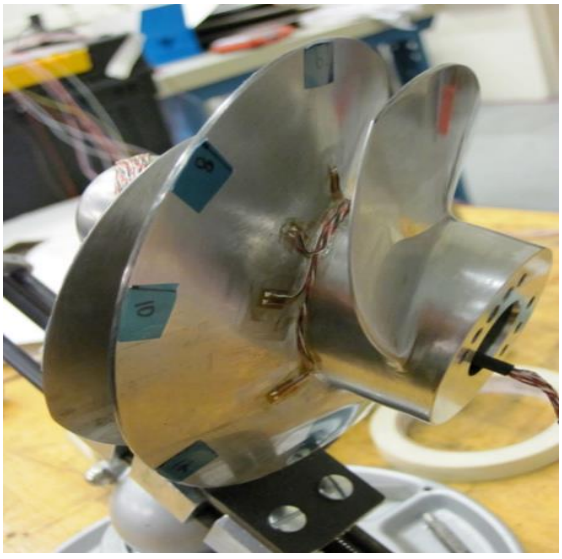

Fig. 1 Typical Rocket Engine Turbopump Inducer (not to scale)

As with most other turbopump inducers, there is some level of cavitation, which is a "phenomenon in which rapid changes of pressure in a liquid lead to the formation of small vapor-filled cavities in places where the pressure is relatively low."[1] The usual problem with cavitation is that these cavities collapse and the liquid then impacts on the blade surface, causing extensive damage, but in the RS-25 inducer, a different type of cavitation field is formed, called "higher-order surge cavitation (HOSC),"[2] which forms an acoustic wave that emanates both upstream and downstream. This wave has been empirically determined to be at a frequency between 6.4 and 6.7 times the engine speed for this inducer, and has a high enough magnitude to resonate with modes of structures impinging on the wave, especially the inducer blades.

It was recognized during the design of the RS-25 that the differing operating conditions would cause operation in HOSC which was not seen during SSME operation. Although no empirical evidence of cracking in this inducer had been seen during testing or operation, this new potentially resonant condition requires structural dynamic assessment for assured safe operation. The assessment requires knowledge of the natural frequency of potentially excitable modes, of course, but in this case a large number of complicating factors cause both considerable adjustment from in-vacuo natural frequencies as well as uncertainty in those adjustments. These include a large adjustment of Young's Modulus of the Titanium alloy used because of operation in a cryogenic (-423°F) environment; the effect of fluid-added mass of the liquid hydrogen; the magnification of this effect due to tight blade tip-clearances with the housing; the effect of structural-acoustic interaction for a slightly compressible fluid; and the effect of multi-phase fluid density where the liquid is cavitating. The magnitude of these adjustments was initially estimated by Aerojet/Rocketdyne (the engine contractor) by using either available test data from similar structures or closed-form, theoretical extrapolations from the underlying physics. The uncertainties in each adjustment, on the other hand, were based purely on subjective "low, medium, or high" confidence levels, which were translated into percentages of the adjustment. As the actual values of the natural frequencies cannot be measured in operation due to the extreme environment and sensitive nature of the hardware, these adjustment and uncertainty estimates play a critical role in qualifying the turbopump for flight. This qualification uses a combination of physics-based and empirically-based techniques which will not be discussed here.

An extensive analytical and testing campaign was initiated in 2017 to help determine these adjustments, as documented by the authors.[3],[4] This campaign consisted of four modal/ping tests of hardware that have some similarity to the actual hardware and in environments that have some similarity to the actual environment. Those performed in LH2 are the first documented in the literature. These tests consisted of the following (Fig. 2):

1) Ping tests in air and LH2 of cantilever beam (CBeam) made of the same Titanium alloy as the actual inducer.
2) Ping test of cantilever beam in LH2 with a tight tip clearance.
3) Modal test of sub-scale inducer with medium tight tip clearance in water.
4) Modal test of stainless steel sub-scale (SS) inducer in air and water, ping test in LH2.

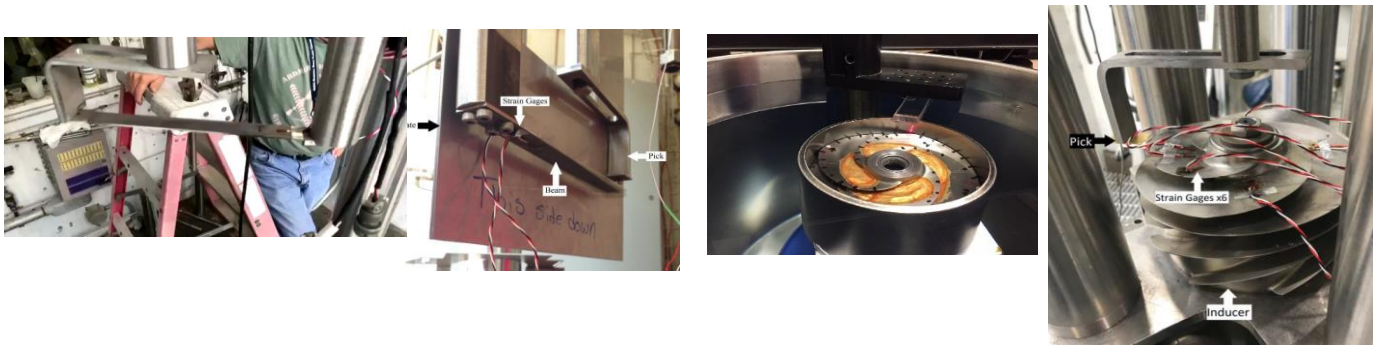

Fig. 2 Modal & Ping Test Series

These tests were largely successful, with consistent results that enabled updates to the adjustments and modeling techniques due to a number of the various effects. In particular, the effect of cryogenic temperatures on the stiffness properties of the Titanium alloy, the effect of fluid-added mass (for both LH2 and water), and the effect of tight tip clearance were refined.

However, it was still unclear how to improve the subjective uncertainty estimates. Table 1 shows the test/analysis error of the updated models, and it is not clear how to implement these into a global uncertainty estimate for a particular effect.

Table 1 Test/Analysis Error Summary

Description	Error analysis from test	Error note	Effect tested
SS Inducer, LH2, open	-3.23%		Fluid Added Mass
SS Inducer, Water, open	-3.70%		Fluid Added Mass
SS Inducer, Water, tight	-1.80%		Fluid Added Mass, Tip Clearance
Ti C beam water, open	0.80%	approximate weighted average of modes	Fluid Added Mass
Ti C beam, water tight	3.00%	approximate weighted average of modes	Fluid Added Mass, Tip Clearance
Ti C Beam, LH2, open	0.80%	approximate weighted average of modes	Fluid Added Mass, E=f(Temp),
Ti C Beam, LH2, tight	2.00%	approximate weighted average of modes	Fluid Added Mass, Tip Clearance, E=f(Temp)

After considerable study, a methodology based on the Bayesian updating of the variance of correlated random variables was identified as a reasonable technique to quantify the total uncertainty in the full-scale operational inducer. In particular, the eigenvalues from the four tested configurations and the untested actual configuration are used as the correlated random variables, and the modal tests give information that can be used with the correlation to infer an improved (reduced variance) posterior distribution of the desired eigenvalue. This application of Bayesian techniques in this way has not been previously presented in the literature, and is the subject of this paper.

LITERATURE SURVEY

An extensive literature survey was undertaken to determine an approach for quantifying the uncertainties of numerous complicating effects on the dynamic characteristics of the full-scale actual inducer. Investigation into implementing this concept led to a vast number of papers on uncertainty quantification (UQ), with a small subset focused on structural dynamics. Atamturktur, et. al.[5] looked at UQ of natural frequencies and modes of the National Cathedral in Washington, D.C., based upon correlation to primitive random variables (rv's), such as material properties, and formulated a Bayesian approach to quantifying inference uncertainty of these properties using Gaussian Process Emulators. The final result was a new posterior distribution of the dynamic characteristics, which is what is being sought here. As with our study, the experiment used to make this updated inference is modal test. The experimental data is used to quantify the primitives, which are then filtered and propagated to obtain the desired output variance. These techniques are also applied to the dynamics of wind turbine blades by Van Buren and Atamturktur.[6] As defined here, inference UQ is the determination of a posterior that "is the probability law that leads to predictions of resonant frequencies that are statistically consistent with the experimental data." In these two papers, the Markov Chain Monte Carlo methodology, which essentially is the development of output statistics by numerous expensive simulations of the finite element models, is replaced by Gaussian Process Emulators. The end result of this model updating process is a non-deterministic model rather than a typical deterministic one. Marwala also uses modal test to update the model via Bayesian updating of the primitive random variables.[7]

Mullins and Mahadevan do not look at structural dynamics specifically, but do generate a Bayesian framework encompassing all of the issues in the discipline, examining differences in propagation for aleatory versus epistemic uncertainties, the impact of sparse data, incorporating experimental results, and examining model-form error. The number of considerations brought up in this paper are somewhat overwhelming, and the techniques necessary to address them are quite advanced.[8]

CONDITIONAL COVARIANCE

As the focus of this study was only to quantify the uncertainty of the final model of the full-scale inducer rather than update the model, which had been previously performed, it was deemed excessively complex to apply the techniques shown in the literature, which focus on improving the primitive random variable posterior distributions and generating non-deterministic models that would then be propagated. The initial concept was generated based on studies by the lead author on identifying the uncertainty in the new NASA Space Launch System Flight vehicle primary mode based upon ground modal testing of the vehicle.[9] In that study, a quartile linear regression technique was used to obtain the flight-mode purely as a regression on a single ground-mode, as opposed to this case where dependence on a number of modes from different configurations was sought.

Here, we have four different modal-tested configurations whose resulting dynamic data could be used to improve the posterior distribution of the full-scale inducer natural frequency of concern. Based upon the papers discussed above, a text on Gaussian processes by Gramacy was examined, which led to the definition of multivariable conditional covariance.[10] Derived from Bayes Theorem, which is

$$p(\theta \mid x) = \frac{p(x \mid \theta)\, p(\theta)}{p(x)} \tag{1}$$

where θ is the parameter being inferred, and **x** is the variable observed experimentally, it states that for a multi-variate random distribution where the random variables are expressed as vector **x**, then this vector can be partitioned into $\mathbf{x}_1$, which are the random variables for which updated statistics are sought, and $\mathbf{x}_2$, which are the random variable which have data that can be used for inference.

$$x = \begin{bmatrix} x_1 \\ x_2 \end{bmatrix} \text{ with sizes } \begin{bmatrix} q \text{ x } 1 \\ (N-q) \text{ x } 1 \end{bmatrix} \tag{2}$$

The means of the rv's are partitioned similarly, and the covariance matrix relating the rv's is partitioned as

$$\Sigma = \begin{bmatrix} \Sigma_{11} & \Sigma_{12} \\ \Sigma_{21} & \Sigma_{22} \end{bmatrix} \text{ with sizes } \begin{bmatrix} \text{q x q} & \text{q x (N-q)} \\ \text{(N-q) x q} & \text{(N-q) x (N-q)} \end{bmatrix} \tag{3}$$

The distribution of $\mathbf{x}_1$ conditional on $\mathbf{x}_2$ equaling **a**, a known vector (in our case, the vector of modal test natural frequencies) is therefore is multivariate normal ($\mathbf{x}_1 \mid \mathbf{x}_2 = \mathbf{a}$) ~N$\left(\bar{\mu}, \bar{\Sigma}\right)$ where

$$\bar{\mu} = \mu_1 + \Sigma_{12}\Sigma_{22}^{-1}(a - \mu_2) \quad \text{and covariance matrix } \bar{\Sigma} = \Sigma_{11} - \Sigma_{12}\Sigma_{22}^{-1}\Sigma_{21}. \tag{4}$$

The concept of how this conditional calculation improves (reduces) the posterior variance is somewhat illustrated graphically in Fig. 4. The multi-variate surface is reduced to a 2-D curve by taking a slice where the information (the modal test natural frequency results) is given. This explains the odd fact that the information from the modal test (i.e., $\mathbf{x}_2 = \mathbf{a}$) is not in the formula for the covariance, which can be understood by realizing that for a multivariate normal, any 2-D slice will have the exact same probability distribution function. Of course, this is based on the assumption of normality, so an error depending on the level of non-normality will exist.

The applicability of eigenvalue covariance as used here to infer a reduction in the posterior variance of a correlated desired output eigenvalue is not conclusive (the authors do not claim to be experts in this complex discipline). However, the methodology was presented to the author of the Gaussian Process text, R. Gramacy, who believed it was legitimate.[11] In addition, although this technique itself was not found in the study of numerous papers, no rejection of the idea was discovered either. Some ideas for technique validation will be proposed in the concluding section of this paper.

APPLICATION OF TECHNIQUE TO PATHFINDER CASE

Although somewhat simplified from more advanced techniques presented in the literature, implementation onto the complex fluid/structure models of the four modal tests as well as the actual inducer was anticipated to be a large challenge. A much simple "pathfinder" case was first processed, therefore, to at least verify the mathematical accuracy of the techniques. The ANSYS™ Workbench and Six-Sigma toolboxes proved critical for enabling the technique. For this case, a cantilever plate in water with a tight clearance from the sides was modeled and a pseudo-modal test value assigned to the first two natural frequencies. A model of a simply-supported plate in water was also modeled, with its fundamental frequency being the sought-after variance to be reduced by conditioning upon the cantilever plate (CP) eigenvalues. The model of the beam, cutaway of the surrounding fluid mesh, and model of the simply-supported plate (SSP) with a partial visualization of the fluid mesh are shown in Fig. 3. After much effort, it was realized that for this technique to work, every conceivable source of error in the modal tested structure (and only those sources) needed to be represented by primitive random variables. Therefore rv's "fluid-added mass (FAM) with tight tip clearance (TC) factor", "cantilever plate geometric imperfection factor (GIF)", and "flat plate geometric imperfection factor" with means of 1.0 and standard deviations of 0.05 were created. The FAM factor was multiplied by the density of the water in both models, and as a simplification on varying the actual geometry, the GIF factors were multiplied by the Young's Modulus of their models.

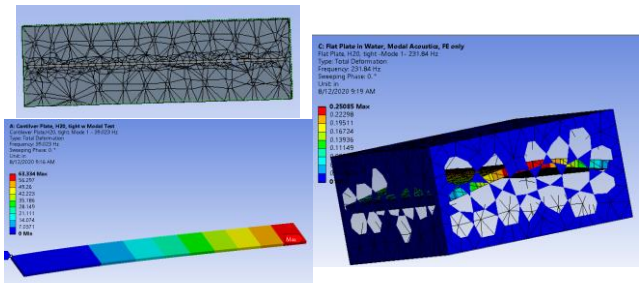

Fig. 3 Cantilever Plate with Fluid Mesh Cutaway, Simply Supported Plate in Fluid

The goal of the process is to generate an accurate covariance matrix relating selected eigenvalues from both systems. Rather than go through the Markov Chain Monte Carlo with the models themselves, which would be completely intractable for the complex inducer system, the ANSYS response surface system methodology is applied. Based upon the variation in the given primitive random variables, a design of experiments set was established to generate the response surface. For each design point, the first two eigenvalues were calculated and a second-order polynomial response surface created. A covariance matrix between all the random variables (primitives as well as eigenvalues) was then calculated by performing a Monte Carlo on the response surfaces 10000 times. Statistics for each rv were also calculated. To ensure that the pseudo modal test value was physically realizable, samples from the primitives were selected and a modal analysis performed to obtain these values for the two cantilever plate modes.

A smaller covariance matrix relating only the eigenvalues was then selected and imported into Matlab, and is shown in Table 2. The means and standard deviations of the eigenvalues as well as the pseudo-modal test values were also input into Matlab and are shown in Table 3. The conditional mean and covariance values were then calculated using equations (4).

Table 2 Eigenvalue Correlation Matrix

CP M1	CP M2	SSP M1	SSP M2
1.0	1.0	.3803	.2995
1.0	1.0	.3565	.2821
.3803	.3565	1.0	1.0
.2995	.2821	1.0	1.0

Table 3 Eigenvalue Initial Statistical Parameters, Modal Test Values, and Conditional Results

Mode	Mean	Coeff Variation	Modal Test
Cant Plate mode 1	39.02 Hz	2.56%	42.991
Cant Plate mode 2	258.01	2.49%	278.52
			Conditional Coeff Variation
SS Plate mode 1	231.9	2.79%	2.40%
SS Plate mode 2	434.33	2.43%	2.24%

For this test case, only a small improvement in the coefficient of variation is obtained, but this is consistent given the poor correlation between the two systems. For illustration, the response surface polynomial was imported into Matlab to enable a separate Monte Carlo analysis to show the correlation between the fundamental modes of each system. A multi-variate normal probability density surface from this calculation for the fundamental modes is shown in Fig. 4, and a red-line identifies the pseudo-modal test value of the cantilever plate. The 2-D PDF curve obtained by slicing the surface at this point will be posterior PDF of the simply-supported plate given only that single input modal test. A great deal was learned from this pathfinder case, particularly the importance of selection of relevant random variables.

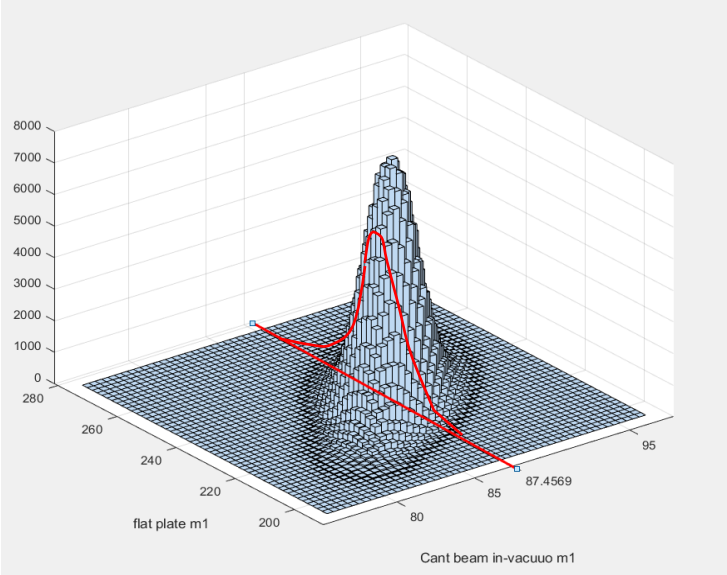

Fig. 4 Multi-variate Normal Probability Density Function with 2-D slice at given information value

APPLICATION OF TECHNIQUE TO INDUCER

As usual, implementation of the technique to the actual inducer case proved orders of magnitude more difficult than for the pathfinder case. Based upon the extensive literature survey and the pathfinder, five primitive random variables were chosen to represent the first three of the modal test configurations (the SS Inducer in LH2 was not used to save modal-tracking review time, which will be discussed below). These primitive random factors are the fluid-added-mass (FAM) effect on liquid density, the tip-clearance (TC) effect on the liquid density, the cryogenic (Cryo) effect on the Titanium alloy, the geometric imperfection effect on the sub-scale Inducer, and the geometric imperfection effect on Titanium tight clearance and open clearance cantilever beams. As with the pathfinder case, the geometric effects are multiplied by the appropriate Young's Modulus. Since the effect on the full-scale inducer

of only the variances for FAM, TC and Cryo are sought, it was decided (after much debate) that a geometric imperfection factor for the FS inducer was not necessary; i.e., the correlation of the FS inducer relative to the modal tested cases needs to include all potential uncertainties in the tested cases but only those effects whose variance will be conditionally inferred in the FS. There is substantial incentive for reducing the number of primitive rv's, as each one doubles the number of design points, but this reasoning may not be rigorous and could lead to error in the results if it is incorrect.

Some simplifying assumptions were made to limit the number of independent primitive rv's. One is that the tip clearance effect factor was assumed to be the same for the SS Inducer in water with a medium tip clearance (see description in reference 4), the cantilever beam in LH2 with a tighter clearance, and the full scale inducer with the tightest clearance. We believe that the acoustic modeling technique for the tight tip regions, which is consistent for all of these models and gave excellent results upon direct test/analysis, will have this same unknown error.

One complicating factor is the modeling of the cavitating region on the full-scale inducer. That has not been discussed in the author's previous papers, and the details will be discussed in a future paper. For now we simply state that there are two cavitating regions on the blade, and different void fractions are assumed for each region. Each of these regions are assumed to have the same effect of uncertainty due to FAM and TC as the non-cavitating regions.

The same general procedure using ANSYS was followed as with the pathfinder. Even though the FS 0ND second bending mode was being sought, it is clear that this mode would be correlated to more than one of the other system's modes, so both the first and second of the cantilever beam modes were chosen as well as the 0ND and 1ND modes of the SS inducer. Upon completion and further understanding of the process, we realize that since these pairs are almost fully correlated to each other, they probably do not yield any additional useful information to the final posterior inference, so could be deleted. In reality, the geometry imperfections might cause different correlations to the FS inducer mode, so if a more precise method of representing that uncertainty was used, the extra mode would be useful. Another way to implement this extra information would be to include a separate modal test error for each mode, but each extra parameter doubles the design points, as noted earlier.

There are two additional severe complications compared to the pathfinder, though. First, the acoustic/structure models are each quite large, and since the five primitives require 54 design points (as determined automatically by ANSYS), the analyses had to be ported from a local computer to a Linux server and then results ported back using the ANSYS RSM utility. As this utility is fairly new, and since the Linux server does not easily run more than a few analyses in parallel, this effort resulted in quite a few failed runs before a step-by-step procedure for running the many design points developed. The second complication was that it was determined that the modes chosen from each model switched in order quite frequently as the primitives were altered from their nominal values in the design points. Although identifying the correct mode potentially could have been performed automatically using a Modal Assurance Criterion calculation, implementing this would have been quite difficult, so instead the modes for each design point were animated and reviewed manually to determine which mode was the correct one to be tracked. The

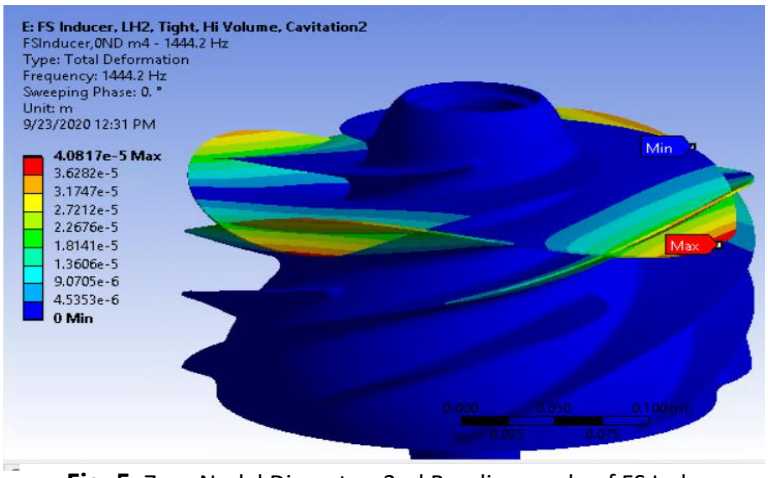

Fig. 5 Zero Nodal Diameter, 2nd Bending mode of FS Inducer (illustration warped).

particular mode shape of the FS inducer is show in Fig. 5. Table 6 shows the information of most of the parameters used in the study (Titanium alloy cryogenic Young's Modulus not shown due to Export Control concerns).

As with the pathfinder case, the correlation matrix was calculated based on the response surface, and so is dependent on the accuracy of the surfaces. Both a full second order polynomial and Kriging fits were attempted. ANSYS enables the creation of a normalized plot of the of the response surface prediction versus actual design point calculation, where the closer the points are to the diagonal the better the prediction is. As the plot for the second order polynomial method shows in Fig. 6, the match is fairly good. A 3D plot of the response surface and design points can also be generated (obviously only 2 of the 5 primitives can be examined on a single plot), and this also shows a good match since most of the points lie on the surface (some of those that don't are hidden) (Fig. 7). The Kriging technique, in contrast, does a better job of matching the surface to the design points, but the response surface has large local warpages to try to match every point, so the second order was chosen as an overall better predictor of the output eigenvalue parameter correlation, which outliers shouldn't overly influence.

CONDITIONAL VARIANCE RESULTS FOR FS INDUCER 0ND MODE

The correlation matrix resulting from the process described results in values shown in Table 7. The results are in the range that would indicate useful answers, as the correlations are good (generally above 0.5) and yet not perfect, which would indicate that uncertainty is not being captured. This matrix and the parameter statistics were input to the Matlab code and the conditional variance calculated as described in the pathfinder case. The results yield a posterior coefficient of variation of the FS Inducer 0ND mode of 0.68%, substantially yet believably improved from the unimproved value obtained directly from propagation of the primitive rv's of 1.18%. While this improvement may not sound noteworthy, it is multiplied by three to incorporate a "three-sigma" overall range, and is double sided, so the actual reduction in uncertainty is 3.02%, which is quite significant in achieving the programmatic goals of the effort. Because of the considerable uncertainties in the methodology itself, this value was compared with the test/analysis errors shown in Table 1 and a rough "upper bound" on uncertainty of 3% is chosen for use in the final inducer assessment. As this value still reduces the original estimated total range of uncertainty by 3%, it is of major value.

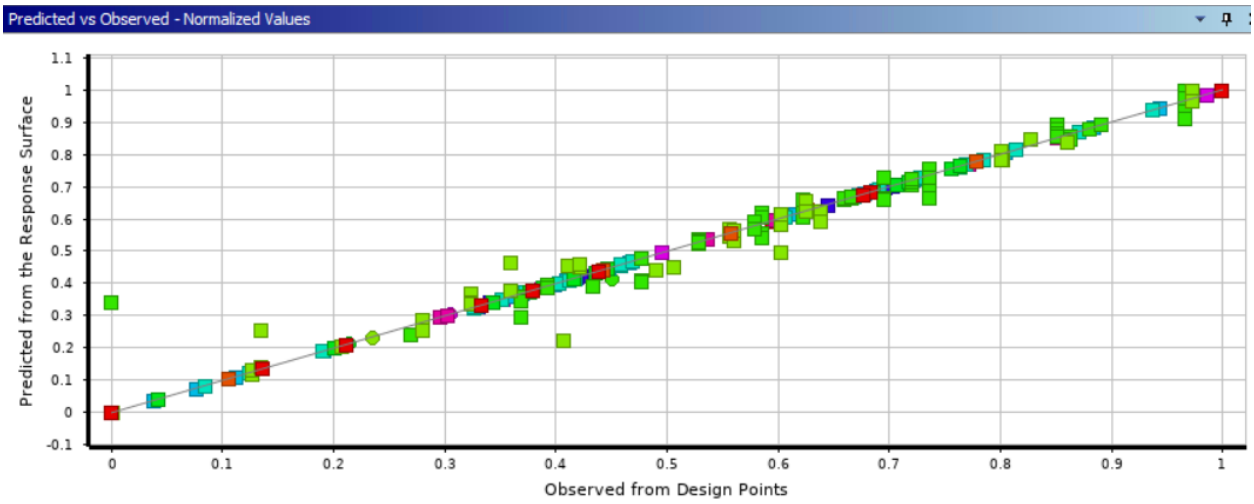

Fig. 6 Matching Capability of 2nd order Response Surface

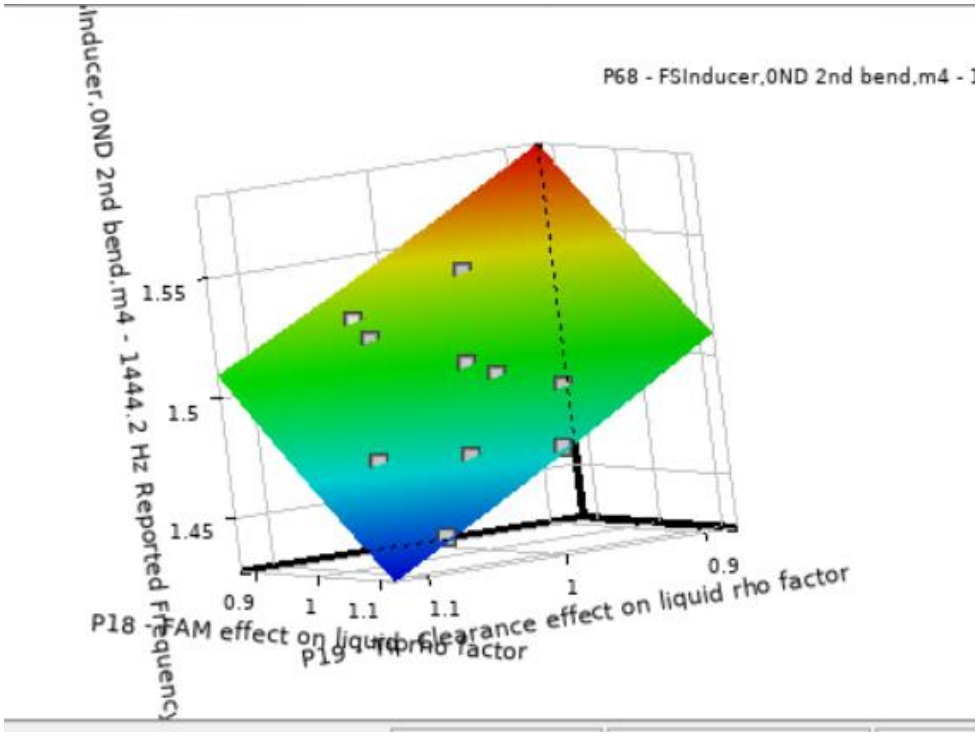

Fig. 7 Response surface for FAM and TC

Table 6 Inducer Parameters

Parameter	Nominal/ Mean Value	Standard Deviation	Modal Test	Notes
FAM effect on liquid density ρ (FAM)	1	.05	Not Applicable	Primitive Random Variable
Tip Clearance Effect on liquid density ρ (TC)	1	.05	NA	Primitive Random Variable
Cryogenic effect on Ti **E** (Cryo)	1	.05	NA	Primitive Random Variable
Geometric uncertainty effect on SS Inducer **E** (GeomSSE)	1	.05	NA	Primitive Random Variable
Geometric uncertainty effect on Cant Beams **E** (GeomCBE)	1	.05	NA	Primitive Random Variable
SS Inducer H2O tight tip clearance ρ* FAM*TC	998.52 kg/m^3	56.323 kg/m^3	NA	Derived Input RV
SS Inducer **E***GeomSSE	2.001e11 Pa	8.0037e9	NA	Derived Input RV
Ti CBeam, Open Clearance LH2 ρ *FAM	70.8 kg/m^3	2.832	NA	Derived Input RV
Ti CBeam, Open, **E***GeomCBE*Cryo	Not shown	Not shown	NA	Derived Input RV
Ti CBeam, Tight Clearance LH2 ρ *FAM*TC	70.8 kg/m^3	3.9935	NA	Derived Input RV
Ti CBeam, Tight Clearance LH2 **E***GeomCBE*Cryo	Not shown	Not shown	NA	Derived Input RV
Full Scale Inducer, tight clearance, non-cavitating region ρ *FAM*TC	70.8 kg/m^3	3.9935	NA	Derived Input RV
FS Inducer, tight LH2 Cavitating region 5% Void Fraction ρ *FAM*TC	67.26 kg/m^3	3.7939	NA	Derived Input RV
FS Inducer, tight LH2 Cavitating region 5% Void Fraction ρ *FAM*TC	63.72 kg/m^3	3.5942	NA	Derived Input RV
SS Inducer H2O tight tip clearance 0ND 2nd bending mode	1477.7 Hz	46.623 Hz	1509.4 Hz*	Output Parameter. *Modal test adjusted by 95.8% to account for not modeling fillet
SS Inducer H2O tight tip clearance 1ND mode	1693 Hz	49.454 Hz	1689.6 Hz	Output Parameter
Ti CBeam, Open Clearance LH2 1st Bending mode	41.182 Hz	1.554 Hz	42.5 Hz	Output Parameter
Ti CBeam, Open Clearance LH2 2nd Bending Mode	259.71 Hz	7.279 Hz	267.5 Hz	Output Parameter
Ti CBeam, Tight Clearance LH2 1st Bending mode	38.437 Hz	1.1013 Hz	40.252 Hz	Output Parameter
Ti CBeam, Tight Clearance LH2 2nd Bending Mode	245.16 Hz	6.9753 Hz	256 Hz	Output Parameter
FS Inducer 0ND 2nd Bending Mode	1505.3 Hz	17.859 Hz	NA	Sought after uncertainty

Table 7 Correlation Matrix for Inducer Systems

Correlation Matrix	P34 - SS Inducer, MedWater,0ND,2ndBend	P35 - SSInducer,MedWater,1ND	P36 - TiCantBeam,Lh2Open,1stBend	P37 - TiCantBeam,Lh2Open,2nd Bend	P38 - TiCantBeam,LH2Tight,1stBend	P39 - TiCantBeam,LH2tight,2ndBend	P68 - FSInducer,0ND 2nd bend
P34 - SS Inducer,MedWater,0ND,2ndBend	1.000	0.871	0.465	0.464	0.590	0.573	0.716
P35 - SSInducer,MedWater,1ND	0.871	1.000	0.588	0.587	0.682	0.668	0.557
P36 - TiCantBeam,Lh2Open,1stBend	0.465	0.588	1.000	1.000	0.979	0.983	0.058
P37 - TiCantBeam,Lh2Open,2ndBend	0.464	0.587	1.000	1.000	0.979	0.983	0.058
P38 - TiCantBeam,LH2Tight,1stBend	0.590	0.682	0.979	0.979	1.000	0.999	0.207
P39 - TiCantBeam,LH2tight,2ndBend	0.573	0.668	0.983	0.983	0.999	1.000	0.188
P68 - FSInducer,0ND 2nd bend	0.716	0.557	0.058	0.058	0.207	0.188	1.000

CONCLUSION AND FUTURE WORK

A new methodology for quantifying the uncertainty of a fundamental natural frequency of a complex, untested system based upon the Bayesian conditional covariance with modal-tested models of simpler systems has been presented. Although intended on being somewhat simpler than other methodologies presented in the literature, the final process was still extremely difficult due to the logistics of running a large number of CPU-intensive simulations and the mode switching. In addition, a number of questions remain on the accuracy of the final variance value obtained, in particular exactly how many and which uncertainties to represent for each configuration, how this value should relate to test/analysis error, and the theoretical accuracy of this methodology in the context of the overall Bayesian UQ hierarchy (as presented by Mahadevan). Nevertheless, if this value is considered along with simple test/analysis errors of the simpler modal-tested systems, the resulting conservative estimate of the variance still has proven to be of tremendous value to the program in assessing the susceptibility of the inducer to possible resonant excitation..

There are a number of possible courses of future work that could help assess the validity of the technique. The most valuable would be to generate a somewhat simpler system of tested structures informing a more complex structure for which the modes could actually be measured; it is not clear to the authors, however, exactly how the uncertainties themselves could be measured for comparison to prediction. In addition, the primitive rv focused methodology described by Atamturktur could be implemented, and the results compared with this eigenvalue covariance conditional technique. Finally, more study on the response surface validation, normality of the multi-variate PDF, and implementation of automatic modal tracking based on the MAC would add information to the validation efforts.

REFERENCES

[1]Wikipedia, “Cavitation,” 4 December 2020
[2] Subbaraman, Maria, Burton, Kevin, “Cavitation-Induced Vibrations in Turbomachinery: Water Model Exploration,” Fifth International Symposium on Cavitation, Osaka, Japan, November 1-4, 2003

[3] Brown, Andrew M., DeLessio, Jennifer L., Jacobs, Preston W., "Natural Frequency Testing and Model Correlation of Rocket Engine Structures in Liquid Hydrogen – Phase I, Cantilever Beam," IMAC-XXXVI Conference and Exposition on Structural Dynamics, Orlando, Florida, February 12-15, 2018, paper 469

[4] Brown, Andrew M., DeLessio, Jennifer L., " Test-Analysis Modal Correlation of Rocket Engine Structures in Liquid Hydrogen – Phase II," IMAC-XXXVIII Conference and Exposition on Structural Dynamics, Houston, Texas, February 10-13, 2020, paper 8732

[5] Atamturktur, S., Hemez, F.M., Laman, J.A, "Uncertainty quantification in model verification and validation as applied to large scale historic masonry monuments," Engineering Structures 43 (2012) 221-234

[6] Van Buren, Kendra L., Molliineaux, Mark G., Hemez, Francois M., Atamturktur, Sezer, Simulating the Dynamics of Wind Turbine Blades: Part II, Model Validation and Uncertainty Quantification," Los Alamos National Laboratory paper LA-UR-11-4997

[7] Marwala, T., Sibisi, S., "Finite Element Model Updating Using Bayesian Framework and Modal Properties," Journal of Aircraft, Vol. 42, No. 1, January-February 2005

[8] Mullins, J., Mahadevan, S., "Bayesian Uncertainty Integration for Model Calibration, Validation, and Prediction," Journal of Verification, Validation, and Uncertainty Quantification, March 2016, 1(1): 011006 (10 pages)

[9] Brown, Andrew M., Peck, Jeffrey A., Stewart, Eric C., "Quantification of Dynamic Model Validation Metrics using Uncertainty Propagation from Requirements," ," IMAC-XXXVI Conference and Exposition on Structural Dynamics, Orlando, Florida, February 12-15, 2018, paper 468

[10] Gramacy, Robert B., Surrogates: Gaussian Process Modeling, Design, and Optimization for the Applied Sciences, CRC Press, 2020, ISBN 9781000766202

[11] Personal Correspondence with Robert Gramacy, August 5, 2020